Atomic and Molecular Resolution Mapping of Solid-Liquid Interfaces by 3D Atomic Force Microscopy

Takeshi Fukuma[†] *and Ricardo Garcia*[*,‡]

[†]Nano Life Science Institute (WPI-NanoLSI), Kanazawa University, Kanazawa 920-1192, Japan.

[‡]Materials Science Factory, Instituto de Ciencia de Materiales de Madrid (ICMM), 28049 Madrid, CSIC, Spain

KEYWORDS. AFM, 3D-AFM, solid-liquid interfaces, hydration layers, atomic resolution, force maps, force-distance curves, force spectroscopy, MD simulations

ABSTRACT. Hydration layers are ubiquitous in life and technology. Hence interfacial aqueous layers have a central role in a wide range of phenomena from material sciences to molecular and cell biology. A complete understanding of those processes requires, among other things, the development of very sensitive and high-resolution instruments. Three-dimensional AFM (3D-AFM) represents the latest and most successful attempt to generate atomically-resolved three-dimensional images of solid-liquid interfaces. This review provides an overview of the 3D-AFM operating principles and its underlying physics. We illustrate and explain the capability of the instrument to resolve atomic defects on crystalline surfaces immersed in liquid. We also illustrate some of its applications to imaging the hydration structures on DNA or proteins. In the last section we discuss some perspectives on emerging applications in materials science and molecular biology.

Interfacial aqueous layers either mediate or play a central role in a wide range of phenomena including wetting, adhesion, corrosion or nanopatterning in material sciences,[1,2] protein stability, folding and molecular recognition in molecular biology[3,4] or growth and dissolution of minerals in geology.[5] Understanding those processes requires the development of very sensitive and high resolution instruments. Those techniques should provide time-resolved three-dimensional images of the interactions occurring between the molecules, atoms, and/or ions forming the solid-liquid interface.

The force microscope (AFM) has transformed the imaging of surfaces by providing real space and atomically-resolved maps of material properties in liquid, air or vacuum. Atomic resolution, operation in different environments and the capability to image organic, inorganic and biomolecules alike are key features of the AFM. Among the surfaces and systems characterized at high resolution by the force microscope are crystalline surfaces and adsorbed molecules in vacuum,[6-8] polymers,[9,11] DNA,[12-14] proteins,[15-17] lipid layers,[18] self-assembled monolayers,[19] 2D layered materials[20,21] or metal-organic frameworks[22] in air or in liquid. In addition, the AFM has imaged protein-protein interactions,[23] the formation of protein assemblies[24] or protein-cell interactions in near-physiological environments.[25] Despite its range of achievements, the AFM has an Achilles' heel. It lacks a genuine three-dimensional depth. This is about to change with the development of the three-dimensional AFM (3D-AFM).[26] This instrument has made possible to image the organization of the atoms, ions, solvent molecules and flexible molecular chains at solid-liquid interfaces.

Figure 1 shows some atomically-resolved 3D images of the local hydration structures observed on different surfaces such as mica (Fig 1a, b) or clinochlore (Fig. 1c). A scheme of the

surface-liquid-tip interface with the presence of solvent molecules and ions (Fig. 1d) and a snapshot of a MD simulation are shown to illustrate the experimental configuration (Fig. 1e).

In 1983, Israelachvili and Pashley reported the first observation on the existence of periodic hydration forces at a solid-liquid interface.[27] They used a surface force apparatus to measure the forces between two macroscopic mica surfaces immersed in dilute electrolyte solutions. Since then, a variety of experimental and theoretical methods have been applied to study interfacial liquids, including the surface force apparatus,[28-30] X-ray reflectometry,[31,32] X-ray absorption spectroscopy,[33] force spectroscopy,[35-38] first-principle and molecular dynamics calculations.[39-42] Those studies provide our current understanding of the structure of solid-liquid interfaces. A liquid near a solid surface forms an interfacial layer where the molecular structure is different from the organization of the liquid molecules in the bulk. The structure and dynamics of the interfacial layer are controlled by the discrete character of the ions and solvent molecules. However, a direct experimental observation of the three-dimensional structure of hydration layers has remained elusive until the development of the 3D-AFM.[26] The observation of atomically-resolved hydration layers on a mica-water interface[26] was either reproduced and/or followed by similar observations on other interfaces.[43-50] The sensitivity and the spatial resolution of the instrument have enabled to extend those observations to non-ideal surfaces such as the ones represented by lipid membranes,[44] proteins[46] or DNA.[50] Those images highlighted a key feature of 3D-AFM, its capability to visualize hydration structures on stiff crystalline surfaces as well as on soft biomolecules.

There are other AFM approaches that claim some three-dimensional depth.[51-57] However, those approaches should not be confused with the 3D-AFM method presented here. First, those approaches aim to image sub-surface structures while 3D-AFM aims to image the organization

of liquid molecules above a solid surface. Second, the imaging mechanisms are different. Lastly, sub-surface AFM methods cannot achieve atomic resolution. Similarly, the 2D *zx* maps of solid-liquid interfaces generated by combining FM-AFM imaging and force spectroscopy[58-60] should be considered as sections of a full 3D-AFM image.

In the last 15 years several AFM-based methods such as topography imaging,[18,19,61-63] force spectroscopy (1D)[34,64-68] and *z-x* mapping (2D)[58-60,69-71] have been applied to study a variety of solid-liquid interfaces and properties. Those contributions have explored several capabilities of AFM to characterize the adsorption of solvent molecules, water and ions on solid surfaces. Many, if not all, the experimental advances achieved by 1D and 2D AFM methods can be incorporated into the 3D-AFM set-ups. In a sense, the successes and limitations to study solid-liquid interfaces at very high spatial resolution have prompted the emergence of 3D-AFM.

This review provides an overview and an outlook to 3D force microscopy by introducing its most relevant instrumental features. Those features are discussed alongside with some applications to understand the structure, dynamics, interactions and composition of aqueous layers on crystalline surfaces, biomolecules or polymers. We also discuss the physical factors that control the observation of atomic-scale corrugation in 3D images. In the process, we address some long standing issues in AFM imaging in liquid. Does the observed contrast represents an intrinsic property of the solid-liquid interface ? Does the tip induce the observed features?

3D-AFM METHODS

In 3D-AFM, the tip is scanned in a synchronized and sequential way in the 3D interfacial space. During each vertical displacement, the force exerted by the tip F is recorded to generate a 3D force map. Several 3D tip scanning and force detection methods have been proposed to realize the 3D-AFM concept (Fig. 2).

3D tip motion. The simplest method is to take multiple force *versus* z-distance curves at 2D-arrayed *xy* positions (Fig. 2a). However, in this 3D approach the imaging is very slow. Hence image distortions caused by the tip or sample drifts are difficult to avoid. This problem is particularly serious for subnanometer-scale resolution experiments. In 2002, Hölscher *et al* presented the first atomically-resolved 3D force mapping on a NiO (001) surface in vacuum.[72] By operating the AFM at low temperatures and using a moderate pixel resolution (32 × 32 × 256 pix^3), they achieved an acceptable imaging rate (80 min/volume) with little image distortion.

An alternative approach to obtain atomic-scale 3D force maps was proposed by Schwarz's group in 2009. This method takes multiple 2D constant height images with different z offsets (Fig. 2b).[73] However, this approach is extremely slow. It took about 40 h to capture a 3D image on a graphite surface with a high pixel resolution (256 × 119 × 60 pix^3). The correlation existing between the 2D images of the surface allowed them to estimate with accuracy the influence of the drifts and compensate for them.[74]

In liquid, non-linear drifts effects are much more evident than in vacuum. The absorption of the liquid by either the substrate or the walls of the liquid cell, sample and/or substrate causes considerable and continuous changes in the relative separation (drifts) between tip and sample surface. Thus, the acquisition of a 3D image at a rate slower than 1 h/image is not acceptable for most solid-liquid applications. In 2010, Fukuma *et al* presented the first atomic-scale 3D force

mapping of a solid-liquid interface by modulating the *z* tip position with a fast sine wave during the slow lateral tip displacement (Fig. 2c).[26] During the scan, the tip-sample distance averaged over the *z* modulation cycle is regulated such that the average value of the main feedback parameter (*e.g*. frequency shift and oscillation amplitude) is kept constant. This simple and continuous tip trajectory of the *z* modulation method improved the imaging speed (53 s/volume, 64 × 64 × 155 pix^3) and simplified the experimental setup. Therefore, this method is currently widely used by several research groups combined with various force detection schemes.[44,46,47]

Force detection. Dynamic operation and detection modes have been predominantly used for performing subnanometer-scale 3D force measurements in vacuum and liquid. This is mainly because a static mode detection (contact mode AFM) does not allow to measure with accuracy the force *versus z* distance curve in the presence of a force gradient larger than the cantilever spring constant. Among the dynamic detection methods, frequency modulation (FM) detection[75-77] is widely used for 3D-AFM measurements However, other dynamic-mode detection methods such as amplitude modulation (AM)[79,80] and bimodal AFM[81] have also been successfully applied to image 3D solid-liquid interfaces. In 2013, Fukuma and Garcia's groups implemented a bimodal AFM configuration for visualizing the 3D hydration structures on mica and GroELs.[46] In 2014, Kuhnle's group imaged 3D hydration structures on calcite using AM detection[47]. Thus, 3D-AFM operation is compatible with the main dynamic AFM modes (AM, FM and bimodal AFM). The advantages and disadvantages of the different dynamic modes are still under debate.[80-84] However, the above examples illustrate that 3D-AFM can incorporate most of the advanced features of dynamic AFM operation to facilitate the imaging of hydration layers.

Cantilever excitation. Acoustic, magnetic and photo-thermal excitation methods have been applied to excite the microcantilever in liquid.[80, 85] Photo-thermal excitation offers the best

balance between the stability and applicability.[85] It also generates canonical resonance curves that can be directly compared with the theory and allows for accurate measurements of the force. Thus, photothermal excitation have significantly contributed to the expansion of 3D-AFM.

Noise and bandwidth. Measurements of the distribution of hydration forces with subnanometer-scale resolution require a force detection method that has locality and a very high signal-to-noise ratio (SNR). The subnanometer-scale locality is achieved by oscillating a cantilever with a small amplitudes (< 0.5 nm).[86,48] Several In addition, other factors have contributed to improve the SNR in 3D-AFM. The spring constant of the cantilever (k) should be sufficiently larger than the force gradient (k_{ts}) of the attractive sections of the force curve. For an oscillatory hydration force profile, k_{ts} can be as high as 2-3 N/m. Thus, k should be higher than 20-30 N/m. This feature is not only necessary for preventing the tip adhesion to the surface but it is also needed for an accurate conversion of the experimental observables (frequency, amplitude or phase of the cantilever oscillation) into force values. In addition, the minimum detectable force (F_{min}) should be smaller than ~10 pN. This last requirement is almost the same as in 2D atomic-resolution imaging.

In dynamic-mode AFM the ultimate value of F_{min} is determined by the thermal vibration of the cantilever. It does not significantly depend on the force detection scheme. In the case of FM-AFM, F_{min} with the small amplitude approximation is given by[87]

$$F_{\min} = \sqrt{\frac{4kk_BTB}{\pi f_0 Q}} \qquad (1)$$

where k_B, T and B are Boltzmann's constant, absolute temperature and the measurement bandwidth; f_0 and Q are the frequency and quality factor of the cantilever resonance. This

equation shows that F_{min} is determined by the cantilever parameters and the bandwidth. Equation 1 shows that there is a trade-off between F_{min} and B. To achieve a force of 10 pN with a standard cantilever (*e.g.*, NCH from Nanoworld or AC160 from Olympus), the bandwidth should ~100 Hz or less.[87] This requirement is sufficient for obtaining 2D images at 1 image/min. However, 3D imaging at 1 image/min requires a bandwidth higher than 1 kHz even for a pixel size of 64 × 64 pix^2. Therefore, the 3D image obtained with a standard cantilever would not capture all the features of the hydration structure. To overcome this limitation, it has been proposed to use ultra-small cantilevers[87] (*e.g.*, USC from Nanoworld or AC55 from Olympus) with a resonant frequency f_0 (fundamental mode) in the megahertz range. As seen from Equation (1), a higher f_0 provides either a better SNR or enables the use of a wider B. For example, the USC cantilever provides F_{min} values of 1.4 pN and 10 pN, respectively, for B of 100 Hz and 5 kHz. The improvement of the signal-to-noise ratio offered by ultra-small cantilevers has been demonstrated experimentally by comparing the force curves obtained on mica in water with the NCH and USC cantilevers.[87] However, 3D imaging at ~1 image/s as it is predicted for those cantilevers has yet to be demonstrated experimentally.

In general, 3D-AFM imposes more stringent requirements on F_{min} or B than 2D-AFM due to the need of using higher acquisition rates. However, the technical demands for improving the imaging speed are not as high as expected from the significant increase of the data acquisition rate. In 2D-AFM, the image distortion caused by the delay in the tip-sample distance feedback cannot be easily corrected by the post processing. In contrast, distortions in 3D-AFM image caused by the delay in the measurement system can be corrected as they do not depend on the feedback error.

HYDRATION LAYERS ON CRYSTALLINE SURFACES

The first application of 3D-AFM in liquid was the imaging of the interface formed between a cleaved muscovite mica surface and an aqueous solution (phosphate buffered saline (PBS) solutions)[26,88] (Fig. 1a). At that time, mica was the standard sample to test atomic-resolution imaging in liquid by AFM. In addition, mica is one of the most widely investigated minerals as a prototype of various clay minerals. Thus, the understanding of its interfacial structures at the nanoscale has significant importance in several fields such as mineralogy, tribology and nanoscale measurement technology.

Fukuma *et al* 3D-AFM images[26,88] were compared with the data obtained previously by X-ray reflectometry[30] and simulations.[89] They attributed the observed layer-like contrast to the hydration layer and the dot-like contrasts to the adsorbed water molecules on the surface. This result gave an important insight into the discussion on the co-existence of "ice-like" and "liquid-like" water molecules at the mica-water interface. In 2013, Kobayashi *et al* obtained a 3D force image in 1 M KCl solution and confirmed its similarity to the 3D water density map calculated by using the 3D reference interaction site model (RISM). [39,44,90]

Those pioneering works highlighted the potential of 3D-AFM for imaging hydration structures in 3D, however, they also raised some fundamental questions regarding the measurement principle and the spatial resolution. Some issues were focused on the influence of the tip structure, the tip hydration and the interfacial ions on the measured force distribution. In other words, to what extent the observed hydration structures are intrinsic to the surface instead of being induced by the tip?. Another relevant issue concerns the capability of the instrument itself to get atomic resolution images in liquid. To address those issues required detailed comparisons between experiments and simulations. However, the mica-water interface is not

necessarily the simplest system to be modelled in an atomistic simulation. On one hand, the one fourth of the surface Si^{4+} ions are substituted by Al^{3+} ions. This exchange leaves the mica surface negatively charged at local sites. On the other hand, the pH-dependent surface protonations induce complicated surface charge distributions. These difficulties motivated the search for another model system to study solid-liquid properties.

Calcite. Calcite ($CaCO_3$) is one of the most abundant carbonate minerals on the Earth and its growth and dissolution influences the global carbon cycle, climate and landforms. Thus, the calcite-water interface has been widely investigated in mineralogy and environmental sciences. In addition, as calcite is sparingly soluble in water, the cleaved calcite surface is automatically renewed to present an atomically clean surface in aqueous solution. Thus, the calcite-water interface has been intensively investigated by AFM since the early days of the AFM development[91]. In contrast to the mica-water interface, the calcite surface has a uniform stoichiometry and regular charge distribution. Therefore, atomistic simulations of calcite are easier to perform than those for the mica-water interface.

To avoid additional complexities, the first simulation model did not include any ions. Thus, a direct comparison between the simulation and experiments required to perform 3D measurements in pure water. At that time, it was empirically known that atomic-resolution imaging in an ionic solution was more reproducible and stable compared to imaging the same surface in pure water. The reason for this difference is not fully understood, however, , there are some explanations. In an experiment, water cannot be perfectly pure because it contains traces of ions. Thus, ions exist at the interface but their distribution and dynamics are not well-defined. In contrast, in an ionic solution (> 100 mM), the Debye length becomes less than 1 nm and the interface is much more well-defined. In addition, the reduced Debye length supresses the long-

range force applied to the cantilever and the tip sidewalls. These factors could explain the improved stability and reproducibility observed in 3D-AFM experiments performed in salt solutions.

In 2015, Foster and Fukuma's groups reported a combined experimental and simulation study on the structure of hydration layers on calcite[92]. They presented a subnanometer-resolution 3D image obtained in pure water by using an ultra-small cantilever with a resonance frequency of ~3.5 MHz. This frequency was more than 20 times higher than the standard cantilever (~150 kHz). Hence those cantilevers provided a much better sensitivity and an averaging effect of intrinsically stochastic processes at a solid-liquid interface. They compared the 3D images obtained by simulation and experiments. The resemblance between the theoretical and the experimental results provided the theoretical basis to explain the imaging of subnanometer hydration structures with a nanoscale tip having a hydration structure on its own (see below for details).

Beyond standard solutions. The above contributions established mica and calcite as the model surfaces to investigate various interfacial structures and their correlation with hydration structures by 3D-AFM. Thus, the majority of the subsequent works were performed on these surfaces except for a few cases. Some contributions have been focused on investigating the role of ions adsorbed on or embedded in the surfaces and their influence on the hydration structures formed above them. Garcia's group performed 3D force measurements on a mica in a nearly saturated KCl (Fig. 1b) or NaCl solution (3-5 M) and found subnanoscale contrasts with an extraordinary large vertical extent (~3-4 nm).[48] By comparing the experimental results with classical fluid density functional simulations, they attributed the observed well-ordered structures to the alternating cation and anion layers with substantial amount of water included. In a

subsequent contribution, Martinez-Jimenez and Garcia classified the force-distance curves from the 3D force image obtained on a mica in 200 mM KCl solution in two types.[93] The classification enabled them to identify the positions of individual K^+ ions adsorbed on a mica surface.[93] Similarly, Söngen *et al* compared the 3D force images obtained on calcite and dolomite [$CaMg(CO_3)_2$] crystals and discussed the differences observed in the force curves taken on the Ca^{2+} and Mg^{2+} ions and their correlation with the hydration structures.[94] In another contribution, 3D force images were taken on an atomic-scale defect at the calcite surface immersed in water.[95] The comparison between the experimental results and the simulations revealed the existence of irregular hydration structures associated with point defects. In the meanwhile, Miyazawa *et al* reported[96]some differences between the 3D force images obtained on a fluorite surface (CaF_2) in pure water and those obtained in a supersaturated solution of CaF_2. The differences observed in the 3D-AFM images were explained in terms of the changes of the hydration structure caused by the interfacial ions.[96] Other studies investigated the changes of the hydration structure on a calcite surface in supersaturated solution of $CaCO_3$ induced by adding Mg^{2+} or polypeptides.[97]

Lately, 3D-AFM has been applied to study more complicated interfacial structures on crystalline surfaces. Yamada's group investigated the hydration structures formed on a heterogeneously-charged interface.[98] They obtained 3D force images at the boundary between the positively charged brucite-like layer and a negatively charged talc-like layer at the cleaved surface of a clinochlore (Fig. 1c). The images revealed the different hydration structures on each regions as well as at the boundary between them. The same experimental group has also studied the dependence of the 3D hydration structures on the surface structural dimensions from 0 to 2 degrees of freedom[99] Recently, Schlesinger and Sivan reported 3D-AFM images of layers of condensed gas molecules adsorbed on hydrophobic surfaces.[100]

HYDRATION LAYERS ON BIOMOLECULES AND LIPIDS

The presence of water is a prerequisite for life on Earth. The majority of biomolecules (proteins and DNA among them) are inactive in the absence of water. Thus, the interaction of water molecules with proteins (hydration) is critical for their stability and function.[3,4,101]

Imaging at high resolution the hydration structure of a biomolecule on an aqueous environment is more demanding than performing those measurements on a crystalline surface. On one hand, the effective Young's modulus (stiffness) of a protein could be 3 to 4 orders of magnitude smaller than the one of crystalline surface such as mica.[102] This implies that under the same AFM operational parameters, namely the force, larger deformations are produced on the biomolecule and on its hydration structure than on the crystalline surface. On the other hand, the surface symmetries of a crystal favors the adsorption water molecules by forming regular patterns that facilitates their visualization.

Currently 3D-AFM has been applied to measure hydration layers on GroEL patches,[46] DNA[50,103] as well as on lipid layers.[45] These examples illustrate the capabilities of 3D-AFM to provide real space images of the hydration structure and the local electric double layer of biomolecules.

Proteins. Figure 3a shows *xy* and *xz* frames of AFM images obtained on a patch of GroEL proteins in buffer.[46] The *xz* frame was extracted from a 3D-AFM image. Each individual *xz* frame was acquired in 0.66 s while the whole 3D-AFM image was acquired in 42 s. The *xz* cross-sections show the alternation of light and dark stripes that are modulated by the contour structure

of the GroEL protein[104] (~14 nm) (bottom panel in Fig. 3a). The red discontinuous line marks the outer most surface of the protein. The pattern of light-dark stripes has a width of 0.31 nm, a value close to the diameter of a single water molecule (~0.28 nm). This is indicative of the presence of interfacial hydration layers on top of the proteins. In this example, the observable that enables the imaging of the hydration layers is the amplitude of the tip's oscillation. The values of the amplitude in the light stripe associated with the 1st hydration layer is about 90 pm while the amplitude in the nearby dark region is of 80 pm. Those values means that the instrument should be able to detect changes in the amplitude of about 5 pm. Those very small values indicate the high level of instrumental sensitivity needed to perform 3D-AFM experiments on biomolecules. The above images were obtained by operating the 3D-AFM with an amplitude modulation feedback.

Lipid bilayers. Figure 3b shows a 3D-AFM image of an interface of a lipid bilayer consisting of phosphatidylcholine headgroups and acyl chains (DPPC) in a buffer solution[45] (HEPES). The headgroups are tilted with respect to the vertical direction (see scheme). The position of the headgroups and the hydration layer are marked by arrows. In this example, the observable that enables to detect the hydration layers comes from changes in the resonant frequency. Those values once transformed into interaction forces correspond to about 100 pN on the lipid headgroups, 60 pN on the layers where the water density is higher and about 4 pN in the bulk liquid.

DNA. Sivan's group developed a 3D-AM instrument operated in FM mode[105] to map water density changes on a DNA molecule with a lateral spatial resolution of 1 nm.[50] Figure 4c shows a high resolution AFM image of a double-stranded DNA (B-DNA) and a model that highlights the

major and minor grooves, and the phosphate groups along the backbone. There is a very good correlation between the AFM image and the model. Figure 3d shows the hydration structure of a section of DNA molecule. The regions with higher amount of water molecules appear in red. Those regions are mostly located near the DNA grooves. The overall hydration structure on the DNA remains quite stable after taken successive 3D-AFM images although some minor variations are observed (compare panels in Fig. 3d). Those variations were attributed to changes in tip structure during imaging. The spatial distribution of water was identified by plotting the frequency shift of the tip as a function of the position in *xyz*. The regions with higher frequency shifts are indicative of higher values in the density of water molecules.

ATOMIC RESOLUTION CONTRAST

True atomic-resolution images of surfaces, in particular those obtained by FM-AFM in liquid,[86] stimulated the development of simulation methods[39, 41, 106-113] to interpret the atomic-scale features observed in the experiments. Those theoretical contributions aimed to address several complementary questions, among them, the relationship between the experimental observable (force) and the water density or to explain the capability to generate atomic resolution images in liquid.

Theories and simulations. In 2010, Harada and Tsukada[39,106] proposed to use of the 3D-RISM theory[90] to simulate the force-distance curve measurements obtained in liquid. The 3D-RISM method is a molecular theory of solvation that provides a solution of the density distributions by solving some integral equations. Those results suggested that force profiles can be roughly

explained by the overlap between the hydration structures on the tip and those of the sample surfaces. The simulations were obtained by using a simplified tip model. At about the same time, Watkins, Berkowitz and Shluger[107] performed molecular dynamics (MD) simulations to determine the force as a function of the distance between a nanoscale tip and a CaF_2 surface immersed in water. The simulations used explicit atomic-scale models for the tip and the sample. The simulations showed that force measured by the probe comes from the direct interaction of the tip and the surface and the water mediated interaction associated with the water structure around the tip and the surface. The water mediated interaction has three components, tip-water, water-surface and water-water interactions. They also showed that the main features observed in the force-distance curves are dominated by the water mediated interaction.[107] The direct tip-surface interaction only becomes significant for tip-surface distances where the force has already become strongly repulsive. The measured force represents a balance between the potential energy gain and the entropic gain caused by the release of the interfacial water from the tip-sample junction to the bulk.

In 2013, Reischl, Watkins and Foster proposed to use the derivative of the free energy profile as a function of the tip-sample distance as the theoretical parameter to be compared with the experimental force. They compared two methods for calculating free energy profiles from atomistic MD simulations,[41] umbrella sampling and free energy perturbation. Both methods provided equivalent free energy profiles but have different features in terms of efficiency and constraints. The above contributions established the theoretical methodologies for simulating one-dimensional force-distance curves $F(z)$ in liquid.

The first full simulation of a 3D force map in liquid was performed by applying the 3D-RISM method to deduce the forces exerted by a single-wall carbon nanotube on a mica surface in an

environment of water molecules.[106] These simulations provided force maps similar to those obtained experimentally.[26,51] However, the experimental results used for the comparison were obtained in an ionic solution with a hydrophilic Si tip while the simulation was performed in pure water with a hydrophobic carbon tip. In addition, at a mica surface, one-fourth of the Si atoms are randomly replaced with Al atoms. Those factors prevented a detailed experimental and theory comparison.

In 2015 it was reported a direct comparison between experimental 3D force maps and those obtained by MD simulations of a calcite-water interface.[92] The simulations and the experiments were performed in pure water by using a hydrophilic tip. The simulations reproduced the alternating peaks observed on Ca and CO_3 sites. The conclusions were based on the analysis of the changes in the hydration structure around the tip apex during the tip approach to the surface. It was established that the events happening at the gap between the tip front atom and the surface topmost atom are the ones that predominantly influence the subnanometer-scale variation of the free energy of the system and, consequently, the force applied to the tip. The regions of the nanoscale tip outside the gap might cause some minor changes in the background values of the long-range force. Those regions could also disturb the hydration structure in a larger scale. However, those effects hardly influence the subnanometer-scale contrast observed in the force. These findings provided a qualitative answer to one of the most fundamental questions on the imaging mechanism: why the subnanometer-scale contrast observed in 3D-AFM is similar to the intrinsic 3D hydration structure (in the absence of the imaging tip).

MD simulations that include an explicit tip model play an essential role in understanding the features observed in 3D-AFM images. However, it is unpractical to apply the same method for analysing all the experimental data because those MD simulations demand large

computational costs. In practice, the AFM data obtained in liquid are often compared with MD simulations that do not introduce the tip.[19,42,48,113-116] However, the water density profiles derived from simulations without a tip[42,44,48] and the 3D-AFM data, in particular, the force-distance curves experiments are expressed in terms of different physical quantities.[26] As a consequence, those comparisons offer, at their best, a semi-quantitative description of the experiment. In addition, even a qualitative comparison of the image contrast has uncertainty because it is not clear whether the water density map should always show a spatial distribution similar to that of a force map.

The solvent tip approximation. To address the latter issue, a simplified model of the measurement system and a formula describing the relationship between the water density and the measured force was needed. In 2013, Watkins and Reischl[108] and Amano *et al* [109] proposed independently some expressions to link force and water densities. In particular, the solvent tip approximation (STA) model was introduced.[95] In the STA model, the tip is approximated by a single solvent molecule and the force applied to the tip *F(z)* is described by the following equation[108]

$$F(z) = \frac{k_{\mathrm{B}}T}{\rho(\mathrm{z})}\frac{\mathrm{d}\rho(\mathrm{z})}{\mathrm{d}z} \qquad (2)$$

z, k_{B}, T and ρ denote distance between the vertical tip position, Boltzmann's constant, absolute temperature and water density, respectively. This equation allows us to convert the water density maps obtained from MD simulations into force maps which can be compared with the experimental 3D force maps.

Comparison theory and experiments. The STA model introduces a very simplified representation of the tip (a solvent molecule). This simplification with respect to a realistic tip demands to verify its accuracy and limitations in practical applications. To address this issue, Miyazawa *et al* performed a comparative study of three physical parameters of a 3D fluorite–water interface.[117] The side view of the fluorite (111) shows Ca^{2+} and F^- ions (Fig. 4a). Among the F^- ions some are higher F_h and other F_l lower than the Ca^{2+} ions.

The comparison involved the water density map obtained by the MD simulation ρ (x, y, z) (Fig. 4a), the force map F_{STA} (x, y, z) obtained by the STA model (Fig. 4b), and the experimental 3D force map F_{exp}(x, y, z) (Fig. 4c). To simplify we only present the comparison in a xz plane. Similar qualitative features appear in both ρ and F_{STA} such as the layer-like distributions of S4 (density map) and F4 (force map). Again, a good qualitative agreement appears in some localized distributions of water molecules (S1-S3) and forces (F1-F3). However, a closer inspection reveals that the water density map does not exactly show the same contrast than the force maps (*e.g.* S3' in Fig. 4a and F3' in Fig. 4b). Those differences arise when there is a low density spot in the hydration structure due to the atomic-scale surface corrugations. On the other hand, the F_{STA} map has a good agreement with the F_{exp} map in both the layer-like distribution (F4) and the localized distributions of F1-F3 (Fig. 4c). Overall, the correlation observed between the F_{STA} (x, z) and F_{exp}(x, z) maps is higher than the one showed by any of the force maps and the water density. Figure 4d illustrates that the 3D force maps depend on the solvent concentration. This dependence has yet to be simulated by MD.

Force-distance curves. To appreciate the usefulness and limitations of the STA model to interpret the atomic-scale contrast obtained in 3D-AFM images, let's explain the main regions of a generic force-distance curve obtained by 3D-AFM (Fig. 5a). The force-distance curve shows

an oscillatory behaviour that alternates regions of attractive and repulsive forces until the tip establishes a mechanical contact with the surface. From then on the force becomes increasingly repulsive by approaching the tip.

Figure 5b shows a realistic scheme of the surface-liquid-tip interface deduced from MD simulations for the different regions of the force-distance curve. In the image, T0 refers to tip apex atom; T1 to the water molecule adsorbed on T0; S1 refers to the water molecule attached to the sample surface. Figure 5c shows the representation of the same interface as given by the STA model.

In a real experiment, a hydrophilic tip is typically used and hence the local hydration peak under the tip apex plays a critical role in the contrast formation. MD simulations show that in regions marked as (i), (ii), (iii) and (iv) in Fig. 5a, the variations in the force applied to the tip within the subnanometer-scale range are predominantly caused by the variations in the force applied to the hydration peak under the tip apex atom. This is nearly equivalent to the force calculated by the STA model, where an AFM tip is modelled as a single solvent molecule. Thus, F_{STA} shows a good agreement with F_{exp}. From this relationship, it is also clear that the STA model does not work when the last water layer between the tip and the sample is removed (region (v$'$) in Fig. 5a and b).

In an experiment two different situations could happen regarding the last hydration layer. If the hydration structure and the tip apex structure are both relatively stable, a hydration layer remains confined between tip and surface (scheme (v) in Fig. 5b). The force gradually increases due to deformation of the sample and the confinement of S1. The STA model can describe this situation. However, if the tip apex structure is more flexible, the last water layer could be

removed by decreasing the tip-sample surface separation. This leads to a decrease of the force (scheme (v)' in Fig. 5b). By keeping pushing the tip towards the sample, a direct repulsive force between the tip front atom and the surface atom will appear. In such a case, a MD simulation that includes the tip is necessary to describe properly the 3D-AFM experimental maps.

Equation 1 is valid to transform water density values into forces. However, the inverse conversion, this is, to transform force profiles into the water density profiles enhances significantly the errors contained in the experimental force values. More specifically, in an experiment the dependencies of the frequency, the amplitude and/or the phase shift *versus* distance are recorded and converted into force profiles. The force reconstruction process involves an integration of the observables along the tip's trajectory.[118-120] The integration generates some numerical errors. In addition, to get the density by inverting Eq. (2) involves to deal with an exponential function and to perform another integration. Thus, even a slight *dc* offset on the experimental data will be extremely enhanced in the water density profile. For those reasons, the inverse conversion is not recommended.

A more sophisticated conversion theory based on the statistical mechanics of liquids has been proposed.[109] In this method, the tip is modelled as a hard rod ended in a hemispherical apex. The experimental verification of the method has been reported only for 1D force-distance curves. Although this conversion takes much longer time than that by the STA model, future improvements in the computational technology and the implementation method will enable its application to a full 3D data.

True atomic resolution. The capability of 3D-AFM measurements to resolve a point defect in solution was first addressed theoretically[121] and later tested experimentally.[95] Atomistic

molecular dynamics and free energy calculations predicted the capability of the AFM to imaging vacancies and ionic substitutions in the calcite surface in water. Specifically, the imaging of point defects such as Ca or CO_3 vacancies and a Mg substitution. This prediction has been confirmed experimentally.[95] Söngen *et al* compared the 3D force maps obtained by simulations with the 3D-AFM images around a point defect and confirmed that the defect can disturb the hydration structure with a lateral extent of approximately one unit cell.[95] Furthermore, the experimental 3D force data obtained around the defect was subsequently analysed by Li *et al* [122] using an information technology tool referred as the graph-bootstrapping method, where the force profiles constituting the 3D image were automatically categorized to show atomic-scale irregularities.

CONCLUDING REMARKS

Three dimensional AFM has enabled the imaging of hydration structures on several solid-liquid interfaces. Two features set this method apart from other techniques devoted to study solid-liquid interfaces. First, 3D-AFM provides sub-1 nm spatial resolution images of the interface. Second, it has a genuine 3D depth. The latter feature enables the imaging of the average positions of ions and solvent molecules across the interface. The method has already revealed uncharted properties of some solid-liquid interfaces. At high molarities, the interface of mica and aqueous solutions of NaCl or KCl exhibit an organization that extends several nm into the salt solution. 3D-AFM has also revealed insights on how atomic resolution is achieved in a liquid. It also revealed that stable hydration layers can be formed even on a soft biological surfaces where the surface structures are thermally fluctuating.[46,50] Those features underscore a wide range of

potential applications in tribology, catalysis, molecular and cell biology. For example, it could be used to address the molecular origin of the Hofmeister series effect or how the solubility of proteins is affected by the interactions of ions, polar residues and water molecules.[123] It could be also applied to determine which type of cations enter the grooves of the DNA. However, the expansion of the 3D-AFM into those areas faces several scientific and instrumentation challenges.

The majority of 3D-AFM studies have been performed on hydrophilic interfaces. The emergence of materials and devices that involve the use of 2D layered materials[124,125] which in many cases are hydrophobic has introduced additional solid-liquid interfaces for 3D-AFM studies.

Imaging speed. Currently**,** the acquisition of an image of a 5 × 5 × 2 nm^3 volume takes about 90 s. This time should be reduced significantly to track the motion and interactions of ions, solvent molecules and small nanoparticles with different solid surfaces. The incorporation of very small cantilevers with high resonant frequencies together with technologies developed for high speed AFM imaging[126,127] can be useful to reduce the acquisition time. In particular, the recently developed high-speed FM-AFM has enabled true atomic-resolution imaging at ~1 frame/s in liquid.[128] Such technologies could enable the generation of time-resolved 3D images of various solid-liquid interfacial phenomena such as the dynamic changes of the hydration structures and the ion distribution caused by the crystal growth or self-assembly.

***z*-depth.** The largest z-depth achieved in a 3D-AFM image was of 10 nm.[48] Most commonly, 3D-AFM images involve 1 nm depths. Those *z*-depths are well suited to study the adsorption of ions and solvent molecules on atomically flat surfaces. However, they are very small to apply 3D-AFM to imaging the hydration structures of non-flat systems such as nanostructured

surfaces, isolated proteins or cells. Increasing the *z*-depth is also important for applying 3D-AFM to the investigations on 3D distributions of flexible molecular chains such as intrinsically disordered domains of proteins.

Data processing and size. The computer memory needed to save a 3D image is larger than the one needed to store a standard AFM image. The 3D data has been increased by the number of pixels of *z*-depth. In addition, the incorporation of fast acquisition methods will generate a large number of images that will demand the use of powerful computers which are uncommon in AFM. The size and the storage of the 3D files could be simplified by using parametric approaches such as the one implemented in bimodal AFM[129] and/or by introducing big data tools.[130]

Theory and experiments. The interpretation of the 3D features observed in some atomically-resolved 3D-AFM images has been made possible by the introduction of powerful MD simulations and the force-water density conversion theory. However, there is still gap between the knowledge provided by current theoretical models and the experimental observations. The theoretical contributions have been mostly focused on the measurements performed in pure water on a rigid and uniform surface. Therefore, many issues still remain to be investigated on the measurements under more complicated conditions. Some major issues include the theoretical treatment of ions and their influence on the force contrast; to include flexible surface and tip structures. To address these problems, the feedback between theory and experiment must be expanded beyond image resolution to other realms such as big data processing and feedback operation modes.

Combination with other probe methods. A full 3D characterization of solid-liquid interfaces requires the characterization of different charge screening and electrochemical processes. The capabilities of 3D-AFM can be enhanced by incorporating electrostatic[131] and Kelvin probe[132,133] methods.

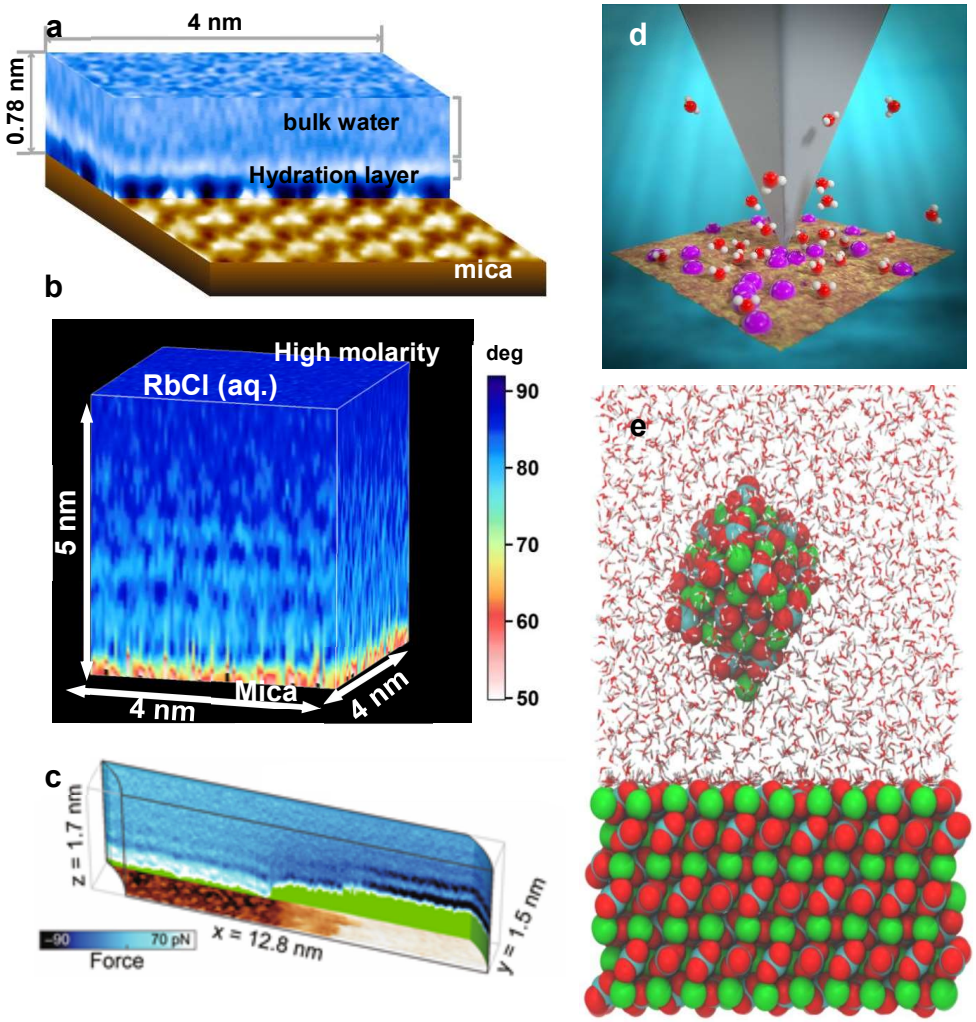

Figure 1. 3D-AFM images and models of solid-liquid interfaces. (a) 3D-AFM map obtained on a mica surface immersed PBS. Adapted with permission from ref 88. Copyright 2010 Japanese National Research Institute. (b) 3D-AFM map of mica immersed in a 6 M RbCl solution. Adapted with permission from ref 48. Copyright 2016 Springer Nature. Here the *z*-depth is obtained by plotting the changes in the tip's phase shift as a function of the spatial coordinate (*x*,*y*,*z*).(c) 3D-AFM force map of a clinochlore surface in a 100 mM KCl aqueous solution. The 3D image shows the local hydration structures at the boundary edges between two terraces. Adapted with permission from ref 98. Copyright 2016 Springer Nature. (d) Schematic view of a tip immersed in a liquid near a solid surface. The liquid includes solvent molecules (far less than in a real experiment and ions. (e) MD snapshot of a calcite-water-tip interface. The tip is simulated by a calcite nanoparticle. The oxygen and the hydrogen of the water molecules are depicted in red and white respectively. The calcium (green) and carbonates (red/ light blue) of the calcite crystal are visible. Reproduced with permission ref 92. Copyright 2015 American Physical Society.

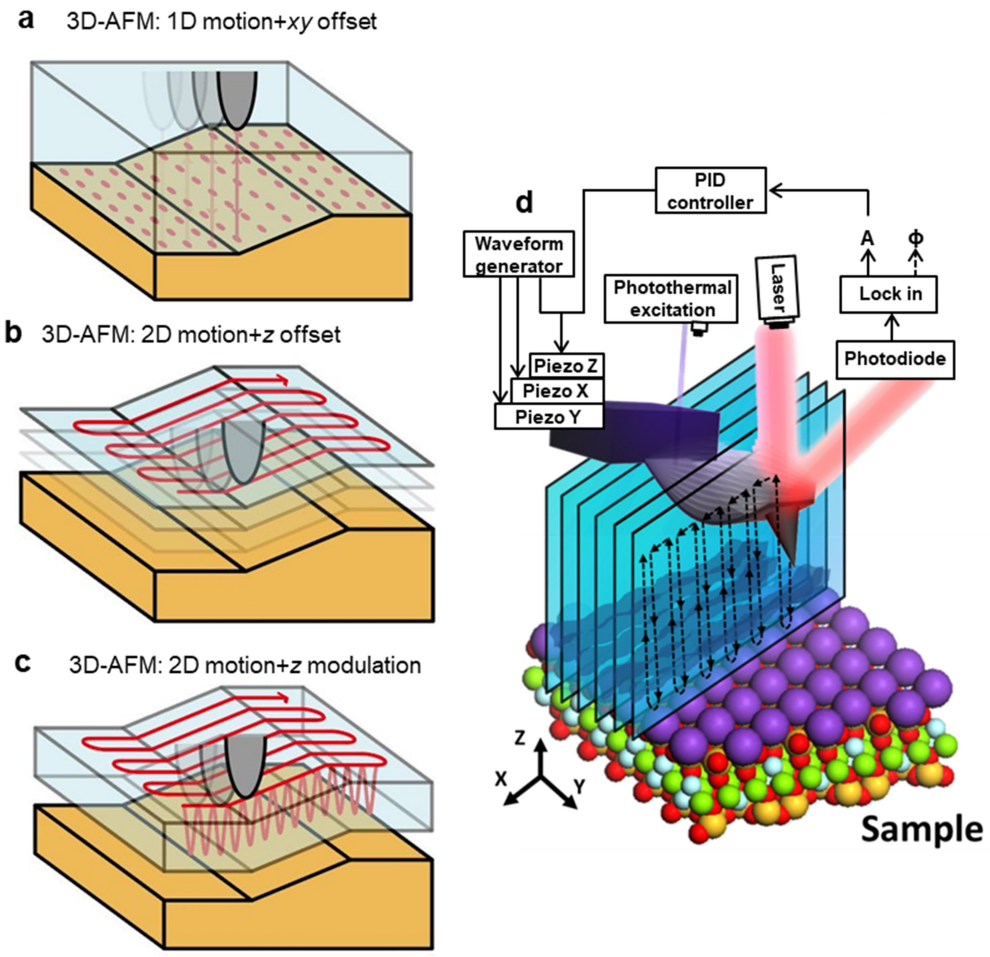

Figure 2. 3D-AFM tip scanning modes. (a). A 3D image is formed by moving the tip in *z* at a fixed *xy* position (1D). Then, the process is repeated for different *xy* positions. (b). A 3D image is formed by scanning the tip in a *xy* plane at a given z value. Then, the process is repeated for different *z* values. (c). A 3D image is formed by scanning the tip in *xy* while the tip-surface distance z is modulated. Panels b-c are adapted with permission from ref 26. Copyright 2015 American Physical Society. (d) Full scheme of a 3D-AFM (2D tip scanning mode and z modulation), cantilever excitation and detection and observables used to acquire a 3D image of a solid-liquid interface. In this scheme the 3D-AFM is operated in the AM mode. Reproduced with permission from ref 48. Copyright 2016 Springer Nature.

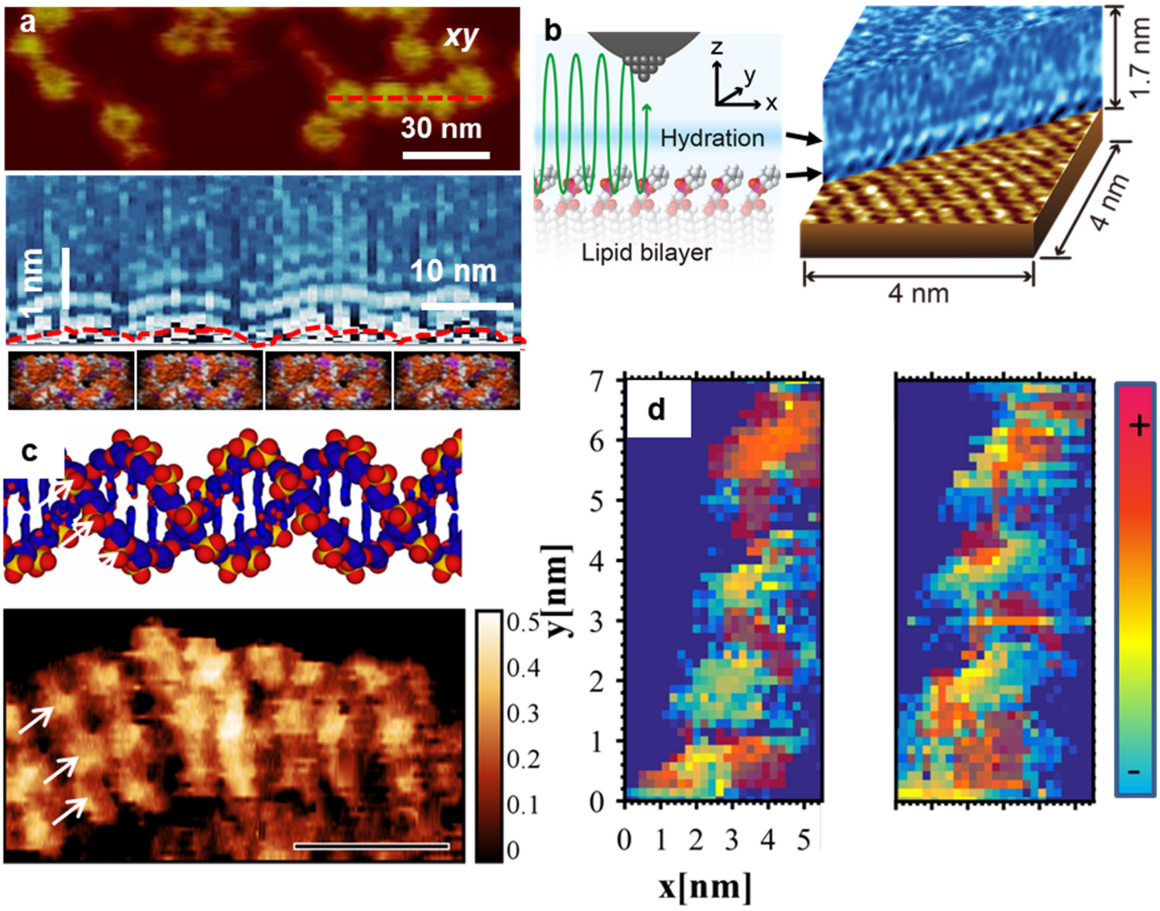

Figure 3. 3D-AFM images of the hydration structure of some biomolecules and lipids. (a) Top panel, AFM image (topography) of the surface of Image of a patch of GroEL molecules in liquid. Middle, *xz* frame of a 3D AFM image of a GroEL-water interface. The red discontinuous line marks the position of the GroEL surface. Adapted with permission from ref 46. Copyright 2013 Royal Society of Chemistry. Bottom, side views of the GroEL structure as obtained by diffraction methods[104] (protein data bank 1KPO). (b) Scheme and 3D-AFM image of a lipid-water interface. Adapted with permission from ref 45. Copyright 2012 American Chemical Society. (c) Scheme and AFM image of a B-DNA molecule. The major grooves and minor grooves are resolved in the image. The top-facing phosphates are highlighted with white arrows on the model and the AFM image. Scale bar: 5 nm. (d). Two hydration images of the same section of a DNA molecule. Pixels shaded red indicate regions with relative high hydration density values. Pixels shaded in blue indicate regions relative low hydration density values. Panels c and d are adapted with permission from ref 50. Copyright 2018 American Chemical Society.

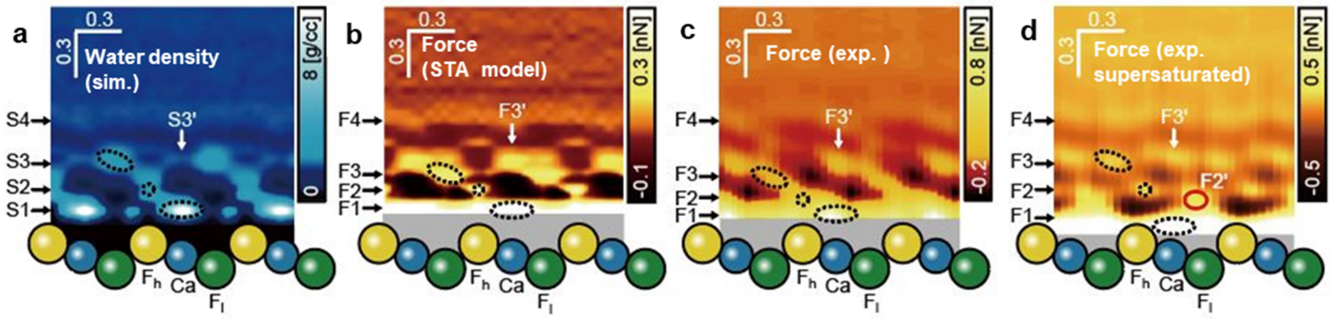

Figure 4. *zx* slices obtained from 3D-AFM images of a fluorite-water interface. (a) Water density map obtained by MD simulations. (b) Force map converted from (a) by applying the STA model. (c) Experimental force map measured of a fluorite-water interface. (d) Experimental force map measured of a fluorite-supersaturated solution of CaF_2. A side view of the last layer of the crystal structure of fluorite (111) is shown at the bottom of the panels. The Ca^{2+} (blue) and F^- ions are indicated. The F^- ions above and below Ca^{2+} are indicated, respectively, as F_h (yellow) and F_l (green). The symbols Sn and Fn (n=1,2,3,4) mark, respectively, different water density and force distributions along the *x* coordinate. Data adapted with permission from ref 96. Copyright 2017 IOP Publishing.

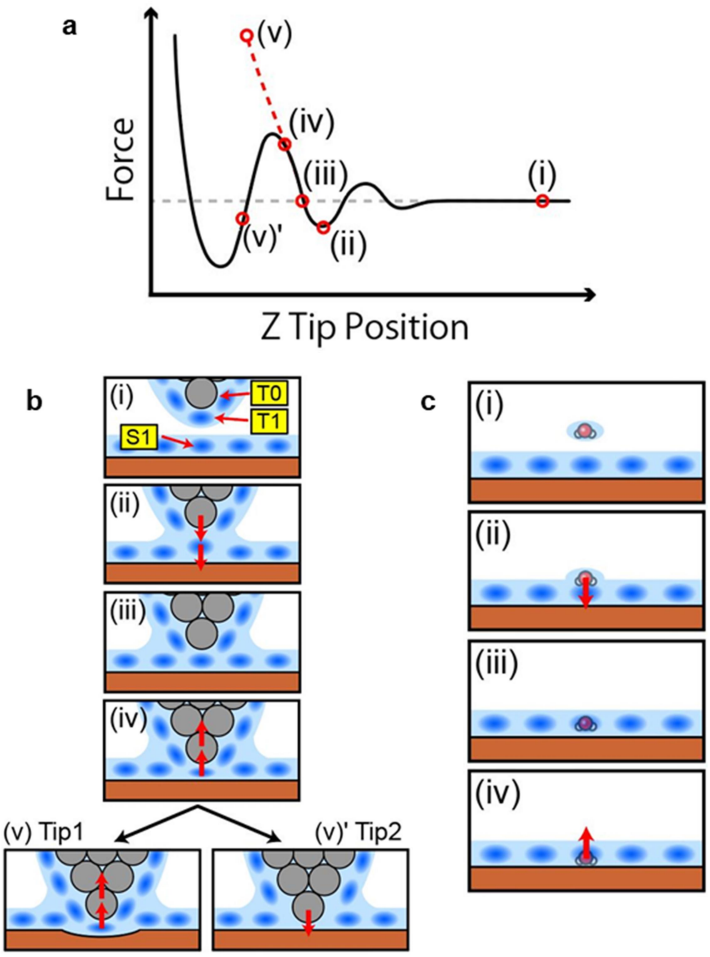

Figure 5. (a) Scheme of the main features of an experimental force-distance curve measured in liquid. Relevant regions of the force-distance curve are marked. (b) Interpretation of (a) in terms of a realistic MD simulation. T0 represents the tip apex atom; T1 is the water attached to T0 and S1 is the water adsorbed on the surface underneath T0. A rigid tip (Tip 1) gives rise to region (v) while a flexible tip (Tip2) gives rise to region (v)′. (c) Interpretation of the features shown in (a) in terms of the STA model. A thick red arrow pointing towards the sample means an attractive force (negative) while a thick red arrow pointing towards the tip indicates a repulsive force. Panels (b-c) are adapted with permission from ref 117. Copyright 2016 Royal Society of Chemistry.

AUTHOR INFORMATION

Corresponding Author

* r.garcia@csic.es

Author Contributions

The manuscript was written through contributions of all authors. All authors have given approval to the final version of the manuscript.

ACKNOWLEDGMENT

TF acknowledges financial support from the World Premier International Research Center Initiative (WPI), MEXT, Japan and JSPS KAKENHI Grant Number JP16H02111. RG acknowledges financial support from the European Research Council ERC–AdG–340177 (3DNanoMech) and the Ministerio de Economia y Competitividad MAT2016-76507-R.

VOCABULARY

Force spectroscopy, a force microscopy-based method to determine mechanical properties from a force-distance curve; **force-distance curve** is the representation of the force sensed by the AFM tip as a function of the tip-surface distance; **topography image** (AFM), the image of the height variations of a surface; **2D image** (AFM), the representation of the force-distance curves contained in a plane perpendicular to the surface; the **hydration layer** is characterized by a layer-like distribution of the water density at the interface between an aqueous solution and a solid surface. The organization of water molecules near a solid surface is different from that of the bulk. The hydration layer could extend about 1 nm from the solid surface; **bandwidth**, the width of the band of frequencies used to process an electronic signal. The information does not depend on where the band is located in the frequency spectrum.

REFERENCES

1 Verdaguer, A., Sacha, G. M., Bluhm, H.; Salmeron, M. Molecular Structure of Water at Interfaces: Wetting at the Nanometer Scale. *Chem. Rev.* **2006**, *106*, 1478-1510.

2. Garcia R.; Knoll, A.W.; Riedo, E. Advanced Scanning Probe Lithography. *Nat Nanotech* **2014**, *9*, 577-87.

3 Mondal, S.; Mukherjee, S.; Bagchi, B. Protein Hydration Dynamics: Much Ado About Nothing ? *J. Phys. Chem. Lett.* **2017**, *8*, 4878-4882.

4 Laage, D.; Elsaesser, T.; Hynes, J. T. Water Dynamics in the Hydration Shells of Biomolecules, *Chem. Rev.* **2017**, *117*, 10694-10725.

5 Laanait, N.; Callagon, E.B.R. ; Zhang, Z.; Sturchio, N.C. ; Lee, S.S.; Fenter, P.. X-Ray-Driven Reaction Front Dynamics at Calcite-Water Interfaces. *Science* 2015, 349, 1330-1334.

6 Ternes, M.; Gonzalez, C.; Lutz, C.P.; Hapala, P.; Giessibl, F.J.; Jelinek, P.; Heinrich, A.J. Interplay of Conductance, Force, and Structural Change in Metallic Point Contacts. *Phys. Rev. Lett.* **2011**, *106*, 016802.

7 Kawai, S. ; Foster, A. S.; Bjorkman, T.; Nowakowska, S.; Björk, J. Canova, F.F.; Gade, L.H.; Jung, T.A.; Meyer, E.. Van der Waals Interactions and the Limits of Isolated Atom Models at Interfaces. *Nat. Commun*. **2016**, *7*, 11559.

8 Gross, L.; Schuler, B.; Pavlicek, N.; Fatayer S.; Majzik, Z.; Moll, N.;Peña, D.; Meyer, G. Atomic Force Microscopy for Molecular Structure Elucidation. *Angew. Chem. Int. Ed.* **2018**, *57*, 3888-3908.

9 Herruzo, E. T.; Perrino, A. P.; Garcia, R. Fast Nanomechanical Spectroscopy of Soft Matter. *Nat. Commun*. **2014**, *5*, 3126-3204.

10 Wang, D.; Russell, T. P. Advances in Atomic Force Microscopy for Probing Polymer Structure and Properties. *Macromolecules* **2018**, *51,* 3–24.

11 Kocun, M., Labuda, A.; Meinhold, W.; Revenko, I.; Proksch, R.. Fast, High Resolution, and Wide Modulus Range Nanomechanical Mapping with Bimodal Tapping Mode. *ACS Nano* **2017**, *11*, 10097-10105.

12 Ido, S; Kimura, K; Oyabu N; Kobayashi, K.; Tsukada, M.; Matsushige, K.; Yamada, H. Beyond the Helix Pitch: Direct Visualization of Native DNA in Aqueous Solution. *ACS Nano* **2013**, *7*, 1817-1822.

13 Ares, P.; Fuentes-Perez, M. E.; Herrero-Galán, E.; Valpuesta, J. M.; Gil, A.; Gomez-Herrero, J.; Moreno-Herrero, F. High Resolution Atomic Force Microscopy of Double-Stranded RNA. *Nanoscale* **2016**, *8*, 11818−11826.

14 Pyne, A.; Tompson, R.; Leung, C.; Roy, D.; Hoogenboom, B.W. Single-Molecule Reconstruction of Oligonucleotide Secondary Structure by Atomic Force Microscopy, *Small* **2014**, *16*, 3257-3261

15 Muller, D.J.; Engel. A. Atomic Force Microscopy and Spectroscopy of Native Membrane Proteins. *Nature Protocols* **2007**, *2*, 2191.

16 Martinez-Martin, D.; Herruzo, E. T.; Dietz, C.; Gomez-Herrero J.; Garcia, R. Noninvasive Protein Structural Flexibility Mapping by Bimodal Dynamic Force Microscopy. *Phys. Rev. Lett.* **2011**, *106*, 198101.

17 Ido, S.; Kimiya, H.; Kobayashi, Kei; Hiroaki, K.; Matsushige, K.; Yamada, H. Immunoactive Two-Dimensional Self-Assembly of Monoclonal Antibodies in Aqueous Solution Revealed by Atomic Force Microscopy. *Nat. Mater.* **2014**, *13*, 265-271

18 Fukuma, T.; Higgins, M. J.; Jarvis, S. P. Direct Imaging of Individual Intrinsic Hydration Layers on Lipid Bilayers at Angstrom Resolution. *Biophys. J.* **2007**, 92, 3603-3609.

19 Kuna, J.J.; Voïtchovsky, K.; Singh, C.; Jiang, H.; Mwenifumbo, S.; Ghorai, P.K.; Stevens, M. M.; Glotzer, S. C.; Stellacci, F. The Effect of Nanometer-Scale Structure on Interfacial Energy, *Nat. Mater*. **2009**, *8*, 837-842.

20 Wastl, D. S.; Weymouth, A. J.; Giessibl, F. J. Atomically Resolved Graphitic Surfaces in Air by Atomic Force Microscopy. *ACS Nano* **2014**, 5233-5239.

21 Korolkov, V.V.; Baldoni, M.; Watanabe, K.; Taniguchi, T.; Besley, E.; Beton, P.H. Supramolecular Heterostructures Formed by Sequential Epitaxial Deposition of Two-Dimensional Hydrogen-Bonded Arrays**.** *Nat. Chem***. 2017**, 9, 1191-1197**.**

22 Amo, C.A.; Perrino, A.P.; Payam, A.F.; Garcia, R. Mapping Elastic Properties of Heterogeneous Materials in Liquid with Angstrom-Scale Resolution, *ACS Nano* **2017**, *11,* 8650.

23 Kodera, N; Yamamoto, D; Ishikawa, R.; Ando T. Video Imaging of Walking Myosin V by High-Speed Atomic Force Microscopy. *Nature* **2010**, *468*, 72-76.

24 Nievergelt, A.P.; Banterle, N.: Andany, S. H.; Gonczy, P.; Fantner, G. E.
High-speed photothermal off-resonance atomic force microscopy reveals assembly routes of centriolar scaffold protein SAS-6. *Nat. Nanotechnol.* **2018,** *13*, 696**.**

25 Dufrêne, Y. F.; Ando, T.; Garcia, R.; Alsteens, D.; Martinez-Martin, D.; Engel, A.; Gerber, G.; Müller, D. J. Imaging Modes of Atomic Force Microscopy for Application in Molecular and Cell Biology. *Nat. Nanotechnol*. **2017**, *12*, 295-307.

26 Fukuma, T.; Ueda, Y.; Yoshioka, S.; Asakawa, H. Atomic-Scale Distribution of Water Molecules at the Mica-Water Interface Visualized by Three-Dimensional Scanning Force Microscopy. *Phys. Rev. Lett.* **2010**, *104,* 016101.

27 Israelachvili, J. N. ; Pashley, R. M. Molecular Layering of Water at Surfaces and Origin of Repulsive Hydration Forces, *Nature* **1983**, *306*, 249-250.

28 Israelachvili, J. N.; Wennerstrom, H. Role of Hydration and Water Structure in Biological and Colloidal Interactions. *Nature* **1996**, *379,* 219-225.

29 Butt, H. J.; Kappl, M. Surface and Interfacial Forces (Wiley-VCH Verlag GmbH & Co. KGaA, Winheim, Germany, 2010).

30 Cheng, L.; Fenter, P.; Nagy, K. L.; Schlegel, M. L.; Sturchio, N. C. Molecular-Scale Density Oscillations in Water Adjacent to a Mica Surface. *Phys. Rev. Lett.* **2001**, *87*, 156103.

31 Fenter, P. ; Lee, S. S. Hydration Layer Structure at Solid-Water Interfaces. *MRS Bull.* **2014**, *39*, 1056-1061.

32 Lee, S. S.; Fenter, P.; Nagy, K. L.; Sturchio, N. C. Real-Time Observation of Cation Exchange Kinetics and Dynamics at the Muscovite-Water Interface. *Nat. Commun*. **2017**, *8*, 15826.

33 Velasco-Velez, J. J.; Wu, C.H.; Pascal, T.A.; Wan, L.F.; Guo, J.; Prendergast, D.; Salmeron, S. The structure of Interfacial Water on Gold Electrodes Studied by X-Ray Absorption Spectroscopy*, Science* **2014**, *346*, 831-834.

34 O'Shea S. J.; Welland, M. E. Atomic Force Microscopy at Solid-Liquid Interfaces. *Langmuir* **1998***,* 14, 4186-4197.

35 Sader, J.E.; Uchihashi, T.; Higgins, M.J.; Farrell, A.; Nakayama, Y.; Jarvis, S.P. Quantitative Measurement of Solvation Shells Using Frequency Modulated Atomic Force Microscopy. *Nanotechnology* **2005**, *16*, S49-S53.

36 Ulcinas, A.; Valdre, GH.; Snitka, V.; Miles, M.J.; Claesson, P.M.; Antognozzi, M.Shear Response of Nanoconfined Water on Muscovite Mica: Role of Cations. *Langmuir* **2011**, *27*, 10351-10355.

37 De Beer, S.; Van den Ende, D.; Mugele, F. Dissipation and Oscillatory Solvation Forces in Confined Liquids Studied by Small-amplitude Atomic Force Spectroscopy. *Nanotechnology* **2010**, *21*, 325703

38 Black, J. M.; Walters, D.; Labuda, A.; Feng, G.; Hillesheim, P.C.; Dai, S.; Cummings, P.T.; Kalinin, S.V.; Proksch, R.; Balke, N. Bias-Dependent Molecular-Level Structure of Electrical Double Layer in Ionic Liquid on Graphite. *Nano Lett.* **2013**, *13*, 5954-5960.

39 Harada, M; Tsukada, M. Tip-Sample Interaction Force Mediated by Water Molecules for AFM in Water: Three-Dimensional Reference Interaction Site Model Theory. *Phys. Rev. B* **2010**, *82*, 035414.

40. Leng, Y. Hydration Force between Mica Surfaces in Aqueous KCl Electrolyte Solution. *Langmuir* **2012**, *28*, 5339-5349.

41 Reischl, B.; Watkins, M.; Foster A. S. Free Energy Approaches for Modeling Atomic Force Microscopy in Liquids, *J. Chem. Theory Comp.* **2013**, *9*, 600-608.

42. Vilhena, J. G.; Pimentel, C.; Pedraz, P.; Luo, F.; Serena, P. A.; Pina, C. M.; Gnecco, E.; Perez, R. Atomic-Scale Sliding Friction on Graphene in Water. *ACS Nano* **2016**, *10*, 4288-4293.

43 Labuda, A.; Kobayashi, K.; Kiracofe, D.; Suzuki, K.; Grütter, P.H.; Yamada, H. Comparison of Photothermal and Piezoacoustic Excitation Methods for Frequency and Phase Modulation Atomic Force Microscopy in Liquid Environments. *AIP Adv.* **2011**, *1*, 022136.

44 Kobayashi, K.; Oyabu, N.; Kimura, K.; Ido, S.; Suzuki, K.; Imai, T.;Tagami, K.; Tsukada, M.; Yamada, H. Visualization of Hydration Layers on Muscovite Mica in Aqueous Solution by Frequency-Modulation Atomic Force Microscopy. *J. Chem. Phys.* **2013**, *138*, 184704.

45 Asakawa, H.; Yoshioka, S.; Nishimura, K. I.; Fukuma, T. Spatial Distribution of Lipid Headgroups and Water Molecules at Membrane/ Water Interfaces Visualized by Three-Dimensional Scanning Force Microscopy. *ACS Nano* **2012**, *6*, 9013−9020.

46 Herruzo, E. T.; Asakawa, H.; Fukuma, T.; Garcia, R. Three-dimensional Quantitative Force Maps in Liquid with 10 Piconewton, Angstrom and Sub-minute Resolutions. *Nanoscale* **2013**, *5*, 2678-2685.

47 Marutschke, C.; Walters, D.; Cleveland, J.; Hermes, I.; Bechstein, R.;Kühnle, A. Three-Dimensional Hydration Layer Mapping on the (10.4) Surface of Calcite Using Amplitude Modulation Atomic Force Microscopy. *Nanotechnology* **2014**, *25*, 335703.

48 Martin-Jimenez, D.; Chacon, E.; Tarazona, P.; Garcia, R. Atomically Resolved Three-Dimensional Structures of Electrolyte Aqueous Solutions near a Solid Surface. *Nat. Commun*. **2016**, *7*, 12164.

49 Söngen, H. ; Marutschke, C.; Spijker, P. ; Holmgren, E.; Hermes, I.; Bechstein, R.; Klassen, S.; Tracey, J.; Foster, A.S.; Kuhnle, A. Chemical Identification at the Solid-Liquid Interface. *Langmuir* **2017**, *33*, 125-129.

50 Kuchuk, K.,; Sivan, U. Hydration Structure of a Single DNA Molecule Revealed by Frequency-Modulation AFM. *Nano Lett.* **2018**, *18*, 2733-2737.

51. Tetard, L; Passian, A; Thundat, T. New Modes for Subsurface Atomic Force Microscopy through Nanomechanical Coupling. *Nat. Nanotech.* **2010**, *5* , 105-109.

52 Spitzner, E. C., Riesch C.; Magerle, R. Subsurface Imaging of Soft Polymeric Materials with Nanoscale Resolution. *ACS Nano* **2011**, *5*, 315-320.

53 Ebeling, D; Eslami, B; Solares, S.D. Visualizing the Subsurface of Soft Matter: Simultaneous Topographical Imaging, Depth Modulation, and Compositional Mapping with Triple Frequency Atomic Force Microscopy *ACS Nano* **2013**, *7* , 10387-10396.

54 Thompson, H. T.; Barroso-Bujans, F.; Gomez Herrero, J.; Reifenberger, R. Raman, A. Subsurface Imaging of Carbon Nanotube Networks in Polymers with DC-biased Multifrequency Dynamic Atomic Force Microscopy, *Nanotechnology* **2013**, *24*, 135701.

55 Bosse, J. L.; Tovee, P. D.; Huey, B. D.; Kolosov, O. Physical Mechanisms of Megahertz Vibrations and Nonlinear Detection in Ultrasonic Force and Related Microscopies. *J. Appl. Phys.* **2014**, *115*, 144304.

56 Gramse, G.; Brinciotti, E.; Lucibello, A.; Patil, S.B.; Kasper, M.; Rankl, C.; Giridharagopal, R.; Hinterdorfer, P.; Marcelli, R.; Kienberger, F. Quantitative Subsurface and Non-contact Imaging Using Scanning Microwave Microscopy. *Nanotechnology* **2015**, *26*, 135701.

57 Van der Hofstadt, M.; Fabregas, R.; Millan-Solsona, R.; Juarez, A.; Fumagalli, L.; Gomila, G. Internal Hydration Properties of Single Bacterial Endospores Probed by Electrostatic Force Microscopy. *ACS Nano* **2016**, *10*, 11327-11336.

58. Kimura, K.; Ido, S.; Oyabu, N.; Kobayashi, K.; Hirata, Y.; Imai, T.; Yamada, H. Visualizing Water Molecule Distribution by Atomic Force Microscopy. *J. Chem. Phys.* **2010**, *132*, 194705.

59. Imada, H;, Kimura, K.; Onishi, H. Water and 2-proponanol Structured on Calcite (104) Probed by Frequency-Modulation AFM. *Langmuir* **2013**, *29*, 10744-10751.

60. Ricci, M.; Spijker, P.; Stellacci, F.; Molinari, J. F.; Voïtchovsky, K. Direct Visualization of Single Ions in the Stern Layer of Calcite. *Langmuir* **2013**, *29*, 2207-2216.

61. Ebeling, D.; Solares, S. D. Amplitude Modulation Dynamic Force Microscopy Imaging in Liquids with Atomic Resolution: Comparison of Phase Contrasts in Single and Dual Mode Operation. *Nanotechnology* **2013**, *24*, 135702.

62. Voïtchovsky, K. Anharmonicity, Solvation Forces, and Resolution in Atomic Force Microscopy at the Solid-Liquid Interface. *Phys. Rev. E* **2013**, *88*, 022407.

63. Ricci, M.; Trewby, W.; Cafolla, C.; Voitchovsky, K. Direct Observation of the Dynamics of Single Metal Ions at the Interface with Solids in Aqueous Solutions. *Sci. Rep.* **2017**, *7*, 43234

64. Li, T. D., Gao, J., Szoszkiewicz, R., Landman, U. ; Riedo, E. Structured and Viscous Water in Subnanometer Gaps. *Phys. Rev. B* **2007**, *75*, 115415.

65. Voitchovsky, K., Kuna J. J., Contera, S. A., Tosatti, E. ; Stellacci, F. Direct Mapping of the Solid-Liquid Adhesion Energy with Subnanometre Resolution. *Nat. Nanotechnol.* **2010**, *5*, 401-405.

66. Ebeling, D.; Van den Ende, D.; Mugele, F. Electrostatic Interaction Forces in Aqueous Salt Solutions of Variable Concentration and Valency. *Nanotechnology* **2011**, *22*, 305706.

67. Kilpatrick, J.I.; Loh, S.H..; Jarvis, S. P. Directly Probing the Effects of Ions on Hydration Forces at Interfaces. *J. Am. Chem. Soc.* **2013**, *135*, 2628-2634.

68. Schlesinger, I.; Sivan, U. New Information on the Hydrophobic Interaction Revealed by Frequency Modulation AFM. *Langmuir* **2017**, *33*, 2485-2496.

69 Suzuki, K.; Oyabu, N.; Kobayashi, K.; Matsushige, K.; Yamada, H. Atomic-Resolution Imaging of Graphite-Water Interface by Frequency Modulation Atomic Force Microscopy. *Appl. Phys. Express* **2011,** *4*, 125102.

70 Spijker, P.; Hiasa, T.; Musso, T.; Nishioka, R.; Onishi, H.; Foster, A. S., Understanding the Interface of Liquids with an Organic Crystal Surface from Atonistic Simulations and AFM Experiments. *J. Phys. Chem. C* **2014,** *118* , 2058-2066.

71 Minato, T.; Araki, Y.; Umeda, K.; Yamanaka, T.; Okazaki, K.; Onishi, H.; Abe, T.; Ogumi, Z. Interface Structure between Tetraglyme and Graphite. *J. Chem. Phys.* **2017,** *147*, 124701.

72 Hölscher, H.; Langkat, S. M.; Schwartz A.; Wiesendanger, R. Measurement of Three-Dimensional Force Fields with Atomic Resolution using Dynamic Force Spectroscopy. *Appl. Phys. Lett.* **2002**, *81*, 4428-4430.

73 Albers, B. J., Schwendemann, T. C., Baykara, M. Z., Pilet, N., Liebmann, M., Altman, E. I. & Schwarz, U. D. Three-Dimensional Imaging of Short-Range Chemical Forces with Picometre Resolution. *Nat. Nanotechnol.* **2009**, *4*, 307-310.

74 Baykara, M. Z.; Schwendemann, T. C.; Altman, E.I.; Schwarz, U.D. Three-Dimensional Atomic Force Microscopy - Taking Surface Imaging to the Next Level. *Adv. Mater.* **2010**, *22*, 2838-2853.

75 Morita, S.; Wiesendanger, R.; Meyer, E. (Eds.): Noncontact Atomic Force Microscopy, Springer-Verlag, 2002.

76 Garcia, R.; Perez, R. Dynamic Atomic Force Microscopy Methods. *Surf. Sci. Rep.* **2002,** *47,* 197.

77 Giessibl, F.J. Advances in Atomic Force Microscopy, *Rev. Mod. Phys.* **2003**, *75*, 949-983.

78 Barth, C.; Foster, A. S.; Henry, C. R.; Shluger, A. L. Recent Trends in Surface Characterization and Chemistry with High-Resolution Scanning Force Methods. *Adv. Mater.* **2011**, *23*, 477-501.

79 Garcia R.; San Paulo A. Attractive and Repulsive Tip-Sample Interaction Regimes in Tapping-Mode Atomic Force Microscopy. *Phys. Rev. B* **1999**, *60*, 4961-4967.

80. Garcia, R. *Amplitude Modulation AFM*; Wiley-VCH: Weinheim, Germany, 2010.

81. Garcia, R.; Herruzo, E. T. The Emergence of Multifrequency Force Microscopy. *Nat. Nanotechnol*. **2012**, *7*, 217-226.

82. Font, J.; Santos, S.; Barcons, V.; Thomson, N.H.; Verdaguer, A.; Chiesa, M. Spatial Horizons in Amplitude and Frequency Modulation Atomic Force Microscopy. *Nanoscale* **2012**, *4*, 2463-2469.

83. Ebeling, D.; Solares, S. D. Amplitude Modulation Dynamic Force Microscopy Imaging in Liquids with Atomic Resolution: Comparison of Phase Contrasts in Single and Dual Mode Operation. *Nanotechnology* **2013**, *24*, 135702

84. Dagdeviren, O.E.; Zhou, C; Altman, E.I.; Schwarz, U.D.. Quantifying Tip-Sample Interactions in Vacuum Using Cantilever-Based Sensors: An Analysis. *Phys. Rev. Appl.* **2018**, *9*, 044040.

85 Fukuma, T**.** Wideband Low-Noise Optical Beam Deflection Sensor with Photothermal Excitation for Liquid-Environment Atomic Force Microscopy. *Rev. Sci. Instrum.* **2009**, *80,* 023707.

86 Fukuma, T.; Kobayashi, K.; Matsushige, K.; Yamada, H. True Atomic Resolution in Liquid by Frequency-Modulation Atomic Force Microscopy. *Appl. Phys. Lett.* **2005**, *87*,034101.

87. Fukuma, T.; Onishi, K.; Kobayashi, N.; Matsuki, A.; Asakawa, H. Atomic-Resolution Imaging in Liquid by Frequency Modulation Atomic Force Microscopy Using Small Cantilevers with Megahertz-Order Resonance Frequencies, *Nanotechnology* **2012,** *23*, 135706.

88 Fukuma, T. Water Distribution at Solid/Liquid Interfaces Visualized by Frequency Modulation Atomic Force Microscopy. *Sci. Technol. Adv. Mater*. **2010**, *11*, 033003.

89. Park, S.-H.; Sposito, G. Structure of Water Adsorbed on a Mica Surface, *Phys. Rev. Lett.* **2002**, *89*, 085501.

90. Imaia, T.; Kovaleko, A.; Hirata, F. Solvation Thermodynamics of Protein Studied by the 3D-RISM Theory. *Chem. Phys. Lett.* **2004**, *395*, 1-6

91. Ohnesorge, F.; Binnig, G. True Atomic Resolution by Atomic Force Microscopy Through Repulsive and Attractive Forces. *Science* **1993**, *260*, 1451-1456.

92. Fukuma, T.; Reischl, B.; Kobayashi, N.; Spijker, P.; Canova, F. F.; Miyazawa, K.; Foster, A. S. Mechanism of Atomic Force Microscopy Imaging of Three-Dimensional Hydration Structures at a Solid-Liquid Interface. *Phys. Rev. B* **2015**, *92*, 155412.

93. Martin-Jimenez, D., Garcia, R., Identification of Single Adsorbed Cations on Mica-Liquid Interfaces by 3D Force Microscopy. *J. Phys. Chem. Lett.* **2017**, *8*, 5707-5711.

94 Söngen, H. ; Marutschke, C.; Spijker, P. ; Holmgren, E.; Hermes, I.; Bechstein, R.; Klassen, S.; Tracey, J.; Foster, A.S.; Kuhnle, A. Chemical Identification at the Solid-Liquid Interface. *Langmuir* **2017**, *33*, 125-129.

95 Söngen, H.; Reischl, B.; Miyata, K.; Bechstein, R.; Raiteri, P.; Rohl, A. L.; Gale, J. D.,;Fukuma, T.; Kühnle, A., Resolving Point Defects in the Hydration Structure of Calcite (104) with Three-Dimensional Atomic Force Microscopy. *Phys. Rev. Lett.* **2018**, *120*, 116101.

96 Miyazawa, K.; Watkins, M.; Shluger, A. L.; Fukuma, T., Influence of Ions on Two-Dimensional and Three-Dimensional Atomic Force Microscopy at Fluorite–Water Interfaces. *Nanotechnology* **2017**, *28*, 245701.

97 Araki, Y., Tsukamoto, K., Takagi, R., Miyashita, T., Oyabu, N., Kobayashi, K., Yamada, H., Direct Observation of the Influence of Additives on Calcite Hydration by Frequency Modulation Atomic Force Microscopy. *Cryst. Growth Des*. **2014**, *14*, 6254-6260.

98 Umeda, K.; Zivanovic, L.; Kobayashi, K.; Ritala, J.; Kominami, H.; Spijker, P.; Foster, A. S.; Yamada, H. Atomic-Resolution Three-Dimensional Hydration Structures on a Heterogeneously Charged Surface. *Nat. Commun.* **2017**, *8*, 2111.

99 Umeda, K.; Kobayashi, K.; Minato, T.; Yamada, H. Atomic-Scale 3D Local Hydration Structures Influenced by Water-Restricting Dimensions. *Langmuir* **2018**, *34*, 9114-9121.

100 Schlesinger, I.; Sivan, U. Three-Dimensional Characterization of Layers of Condensed Gas Molecules Forming Universally on Hydrophobic Surfaces. *J. Am. Chem. Soc.* **2018**, *140*, 10473-10481.

101 Ball, P. Water as an Active Constituent in Cell Biology. *Chem. Rev.* **2008**, *108*,74-108.

102 Amo, C.A.; Perrino, A.P.; Payam, A.F.; R. Garcia. Mapping Elastic Properties of Heterogeneous Materials in Liquid with Angstrom-Scale Resolution. *ACS Nano* **2017**, *11*, 8650.

103 Umeda, K.: Kobayashi, Oyabu, N.; Matsushige, K.; Yamada, H. Molecular-Scale Quantitative Charge Density Measurement of Biological Molecule by Frequency Modulation AFM in Aqueous Solutions. *Nanotechnology* **2015**, *26*, 285103.

104 Wang, J.; Boisvert, D.C.. Structural Basis for GroEL-Assisted Protein Folding from the Crystal Structure of (GroEL-KMgATP)(14) at 2.0 Angstrom Resolution. *J. Mol. Biol.* **2003**, *327*, 843–855.

105 Schlesinger, I.; Kuchuk, K.; Sivan, U. An Ultra-Low Noise Optical Head for Liquid Environment Atomic Force Microscopy. *Rev. Sci. Instrum.* **2015**, *86*, 083705.

106. Tsukada, M.; Watanabe, N.; Harada, M.; Tagami, K. Theoretical Simulation of Non-contact AFM in Liquids. *J. Vac. Sci. Technol. B* **2010**, *28*, C4C1.

107 Watkins, M; Berkowitz, M.L.; Shluger, A.L. Role of Water in Atomic Resolution AFM in Solutions. *Phys. Chem. Chem. Phys.*, **2011**, *13*, 12584–12594

108 Watkins, M.; Reischl, B. A Simple Approximation for Forces Exerted on an AFM tip in Liquid. *J. Chem. Phys.* **2013**, *138*, 154703.

109 Amano, K.; Suzuki, K.; Fukuma, T.; Takahashi, O.; Onishi, H. The relationship between Local Liquid Density and Force Applied on a Tip of Atomic Force Microscope: A Theoretical Analysis for Simple Liquids. *J. Chem. Phys.* **2013**, *139*, 224710.

110 Argyris, D.; Anh, P.; Striolo, A.; Ashby, P.D. Hydration Structure at the alpha-Al2O3 (0001) Surface: Insights from Experimental Atomic Force Spectroscopic Data and Atomistic Molecular Dynamics Simulations. *J. Phys. Chem. C* **2013**, *117*, 10433-10444.

111 Kobayashi, K.; Liang, Y.; Amano, K.; Murata, S.; Matsuoka, T.; Takahashi, S.; Nishi, N.; Sakka, T. Molecular Dynamics Simulation of Atomic Force Microscopy at the Water-Muscovite Interface: Hydration Layer Structure and Force Analysis. *Langmuir* **2016**, *32*, 3608-3616.

112. Hu, X.; Nanney, W.; Umeda, K.; Ye, T.; Martini, A. Combined Experimental and Simulation Study of Amplitude Modulation Atomic Force Microscopy Measurements of Self-Assembled Monolayers in Water. *Langmuir* **2018**, *34*, 9627-9633.

113 Cramer, T.; Zerbetto, F.; Garcia, R. Molecular Mechanism of Water Bridge Buildup: Field-Induced Formation of Nanoscale Menisci. *Langmuir* **2008**, *24*, 6116-6120.

114 Argyris, D.; Ashby, P. D.; Striolo, A. Structure and Orientation of Interfacial Water Determine Atomic Force Microscopy Results: Insights from Molecular Dynamics Simulations. *ACS Nano* **2011**, *5*, 2215-2223.

115 Ricci, M.; Spijker, P.; Voitchovsky, K. Water-Induced Correlation between Single Ions Imaged at the Solid-Liquid Interface. *Nat. Commun*. **2014**, *5*, 4400.

116 Siretanu, I. Ebeling, D,; Andersson, M.P.; Stipp, S.L.S.; Philipse, A.; Stuart, M.C.; van den Ende, D.; Mugele, F. Direct Observation of Ionic Structure at Solid-Liquid Interfaces: a Deep Look into the Stern Layer. *Sci. Rep.* **2014,** *4*, 4956.

117 Miyazawa, K.; Kobayashi, N.; Watkins, M.; Shluger, A.L.; Amano, K.; Fukuma, T. .A Relationship between Three-Dimensional Surface Hydration Structures and Force Distribution Measured by Atomic Force Microscopy. *Nanoscale* **2016**, *8*, 7334-7342.

118. Sader J. E.; Jarvis S. P. Accurate Formulas for Interaction Force and Energy in Frequency Modulation Force Spectroscopy. *Appl. Phys. Lett*. **2004**, *84***,** 1801-1803.

119. Holscher, H. Quantitative Measurement of Tip-Sample Interactions in Amplitude Modulation Atomic Force Microscopy. *Appl. Phys. Lett.* **2006**, *89***,** 123109.

120. Payam, A. F.; Martin-Jimenez, D.; Garcia, R. Force Reconstruction from Tapping Mode Force Microscopy Experiments. *Nanotechnology* **2015**, *26*, 1–12.

121 Reischl, B.; Raiteri, P.; Gale, J. D.; Rohl, A.L.. Can Point Defects in Surfaces in Solution be Atomically Resolved by Atomic Force Microscopy ?. *Phys. Rev. Lett.* **2016**, *117*, 226101.

122 Li, X.; Collins, L.; Miyazawa, K.; Fukuma, T.; Jesse, S.; Kalinin, S. V. High-Veracity Functional Imaging in Scanning Probe Microscopy *via* Graph-Bootstrapping, *Nat. Commun.* **2018**, *9*, 2428.

123. Baldwin, R.L. How Hofmeister Ion Interactions affect Protein Stability. *Biophys. J.* **1996**, *71*, 2056-2063.

124 Jariwala, D.; Marks, T. J.; Hersam, M. C. Mixed-Dimensional Van der Waals Heterostructures. *Nat. Mater*. **2017**, *16*, 170-181.

125 Padmanathan. K.K.; Dattatray J. L.; Hywel M.; Chandra, S. R. Recent Developments in 2D Layered Inorganic Nanomaterials for Sensing. *Nanoscale* **2015**, *7*, 13293.

126 Ando, T. High-Speed Atomic Force Microscopy Coming of Age. *Nanotechnology* **2012**, *23*, 062001.

127 Ando, T.; Uchihashi, T.; Fukuma, T. High-Speed Atomic Force Microscopy for Nano-Visualization of Dynamic Biomolecular Processes. *Prog. Surf. Sci.* **2008,** *83,* 337-437.

128. Miyata, K.; Tracey, J.; Miyazawa, K.; Haapasilta, V.; Spijker, P.; Kawagoe, Y.; Foster, A. S.; Tsukamoto, K.; Fukuma, T., Dissolution Processes at Step Edges of Calcite in Water Investigated by High-Speed Frequency Modulation Atomic Force Microscopy and Simulation, *Nano Lett.*, **2017**, *17*, 4083–4089.

129 Garcia, R.; Proksch, R. Nanomechanical Mapping of Soft Matter by Bimodal Force Microscopy. *Eur. Polym. J.* **2013**, *49*, 1897 – 1906.

130 Kalinin, S.V.; Strelcov, E.; Belianinov, A.; Somnath, S.; Vasudevan, R. K.; Lingerfelt, E. J.; Archibald, R. K.; Chen, C.; Proksch, R.; Laanait, N.; Jesse, S. Big, Deep, and Smart Data in Scanning Probe Microscopy. *ACS Nano* **2016**, *10***,** 9068-9086.

131 Fumagalli, L.; Esfandiar, A.; Fabregas, R.; Hu, S.; Ares, P.; Janardanan, A.; Yang, Q.; Radha, mB.; Taniguchi, T.; Watanabe, F.; Gomila, G.; Novoselov, K.S.; Geim, A.K. Anomalously low Dielectric Constant of Confined Water. *Science* **2018**, *360*, 1339-1342

132 Honbo, K.; Ogata, S.; Kitagawa, T.; Okamoto, T.; Kobayashi, N.; Sugimoto, I.; Shima, S.; Fukunaga, A.; Takatoh, C.; Fukuma, T. Visualizing Nanoscale Distribution of Corrosion Cells by Open-Loop Electric Potential Microscopy, *ACS Nano* **2016**, *10*, 2575-2583.

133 Collins, L.; Kilpatrick, J.I.; Kalinin, S.V.; Rodriguez, B.J. Towards Nanoscale Electrical Measurements in Liquid by Advanced KPFM Techniques: A Review. *Rep. Prog. Phys.* **2018**, *81*, 086101.